Stent coating by electrospinning with chitosan/poly-cyclodextrin based nanofibers loaded with simvastatin for restenosis prevention

Dyhia Kersani, Justine Mougin, Marco Lopez, Stephanie Degoutin, Nicolas Tabary, Frederic Cazaux, Ludovic Janus, Mickaël Maton, Feng Chai, Jonathan Sobocinski, et al.

Stent coating by electrospinning with chitosan/poly-cyclodextrin based nanofibers loaded with simvastatin for restenosis prevention

Authors: Dyhia Kersani[a], Justine Mougin[b], Marco Lopez[b], Stéphanie Degoutin[a], Nicolas Tabary[a], Frédéric Cazaux[a], Ludovic Janus[a], Mickaël Maton[b], Feng Chai[b], Jonathan Sobocinski[b], Nicolas Blanchemain[b] and Bernard Martel[a]*

[a] Univ. Lille, CNRS UMR8207, UMET - Unité Matériaux et Transformations, F-59655 Villeneuve D'Ascq, France

[b] Univ. Lille, INSERM, CHU Lille, U1008 - Controlled Drug Delivery Systems and Biomaterials, F-59000 Lille, France

*Corresponding author: bernard.martel@univ-lille.fr

Graphical abstract

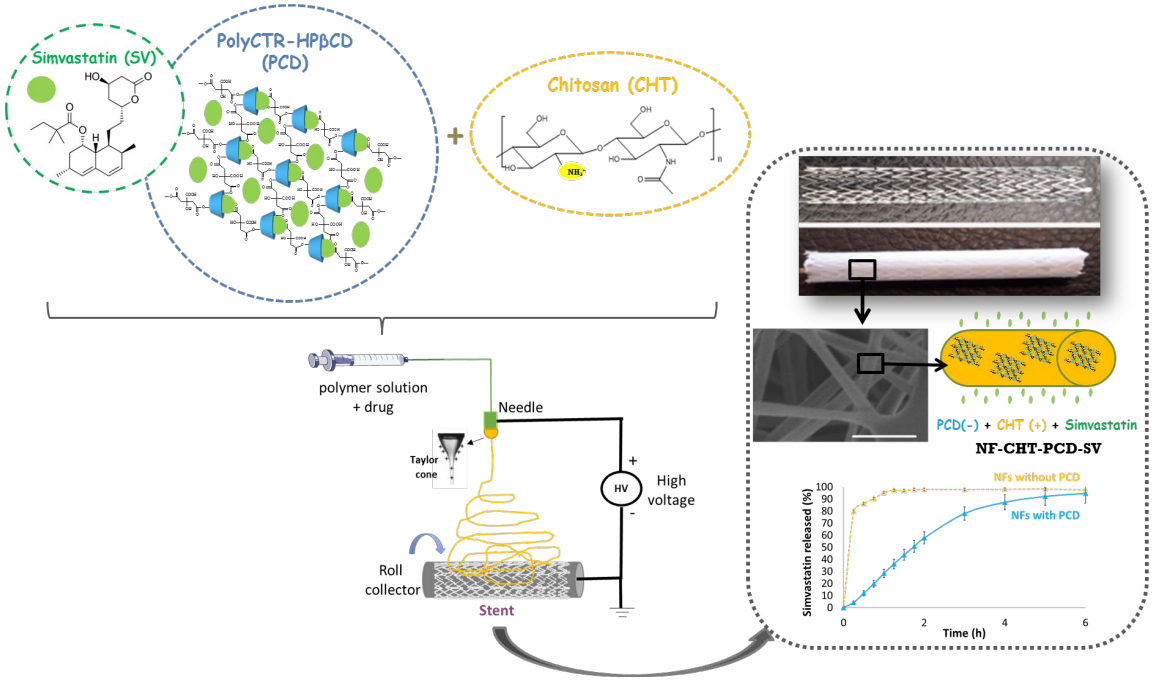

Abstract

The main cause of failure of angioplasty stenting is restenosis due to neointimal hyperplasia, a too high proliferation of smooth muscle cells (SMC). The local and sustained delivery of selective pleiotropic drugs to limit SMC proliferation seems to be the hopeful solution to minimize this post surgery complication. The aim of this study is to develop a stent covered by nanofibers (NFs) produced by electrospinning, loaded with simvastatin (SV), a drug commonly used for restenosis prevention. NFs were prepared from the electrospinning of a solution containing SV and a mixture of chitosan (cationic) and β-cyclodextrin (CD) polymer (anionic) which form together a polyelectrolyte complex that makes up the NFs matrix. First, the SV/CD interactions were studied by phase solubility diagram, DRX and DSC. The electrospinning process was then optimized to cover a self-expandable NiTiNOL stent and the mechanical resistance of the NFs sheath upon its introduction inside the delivery catheter was considered, using a *crimper* apparatus. The morphology, coating thicknesses and diameters of nanofibers were studied by scanning electron microscopy. The SV loading rates on the stents were controlled by the electrospinning time, and the presence of SV in the NFs was confirmed by FTIR. NFs stability in PBS pH 7.4 buffer could be improved after thermal post-treatment of NFs and i*n vitro* release of SV in dynamic conditions demonstrated that the release profiles were influenced by the presence of CD polymer in NFs and by the thickness of the NFs sheath. Finally, a covered stent delivering 3 µg/mm^2 of SV within 6 hours was obtained, whose efficiency will be investigated in a further *in vivo* study.

Keywords: anti-restenosis, drug-eluting stent, simvastatin, electrospinning, chitosan, cyclodextrins, sustained drug release

1. Introduction

Cardiovascular diseases are the most frequent causes of death in developed countries[1]. The main etiology is atherosclerosis, characterized by the formation of atheroma on the wall of arteries causing a partial then a total obstruction of the artery (stenosis then thrombosis)[2]. The conventional treatment is angioplasty-stenting, which consists in a reopening of the arterial lumen to restore blood flow. This treatment was improved by the use of bare metal stents (BMS) to ensure the permeability of the arteries in the long term[3]. Nevertheless, an inflammatory reaction caused by the implantation of the stent leads to a neointimal hyperplasia in 10 - 30 % of cases (restenosis), resulting in the failure of the treatment[4]. In this context, Drug-Eluting Stents (DES) loaded with anti-proliferative drugs as Sirolimus and Paclitaxel were developed[5,6]. Unfortunately, the clinical results were not as good as expected with late acute thrombosis caused by an inappropriate drug release, a non-selectivity of the drug and the inflammatory properties of erodible polymer[7]. In order to improve efficiency of DES and control the drug release profile, biocompatible and biodegradable synthetic or natural polymers were used as surface coating or matrices[8,9]. A randomized study suggested that a biolimus-eluting stent using a biodegradable polymer matrix was safer and more effective than a sirolimus-eluting stent with a durable polymer[10]. Indeed, the nature of the polymer is a key parameter to control the drug release profile, as well as the technique used to coat the stent with the polymer/drug such as electrospinning[11], dip coating and spray coating[12,13,14]. Among these, electrospinning is a versatile technique widely used for biomedical applications to design nanofibers (NFs) and scaffolds for tissue engineering[15,16] and for drug release[17,18,19]. NFs based membranes present porous structure and offer high surface-area-to-volume ratio. Moreover, NFs mimic the structure of natural extracellular matrix and provide good microenvironment for cell adhesion and proliferation[20]. Finally, electrospinning offers high flexibility in the choice of polymers used for drug delivery system[21]. For example, Lee *et al.* developed a covered DES based on poly(D,L)-lactide-co-glycolide (PLGA) NFs to deliver rosuvastatin (5 µg/mm^2). They observed a significant reduction of platelet adhesion and an improvement of *in vivo* re-endothelialization in a rabbit model[22]. In another study, Tang et *al.* reported the fabrication of covered DES based on core-shell drug encapsulated NFs through co-assembly of chitosan (CHT) and paclitaxel[23]. This study exhibited an efficient encapsulation and well controlled release of paclitaxel using core-shell NFs. However, despite the several efforts in the field of DES coated with NFs for preventing restenosis, limited information is available about metallic stents covered by NFs

based on natural polymers with prolonged release of drug. On the other hand, the release profiles from drug loaded NFs can be modulated by changing the technique of drug incorporation: dissolution in the polymer solution[24], coaxial electrospinning[25], or by using drug carrier molecules such as cyclodextrins[26]. Interestingly, cyclodextrins (CDs) and cyclodextrin polymers are widely used as controlled drug delivery carriers thanks to their ability to form reversible inclusion complexes with lipophilic drugs due to their hydrophobic cavities, and thus enhance the solubility and bioavailability of some hydrophobic drugs[27,28,29,30]. In a previous study, we reported the functionalization of CoCr vascular stent with hydrophilic, biocompatible and biodegradable cyclodextrin polymer for sustained release of paclitaxel (7 days) to prevent restenosis[31]. In addition, the anionic character of citric acid-cyclodextrin polymer (named herein PCD) is adequate to form stable polyelectrolyte complexes with cationic polysaccharides such as CHT[32,33,34]. We previously investigated systems based on polyelectrolyte complex formed between CHT and PCD using layer-by-layer deposition[35,29,36,37], hydrogel and sponge formation[38,39] and electrospinning[40]. In the latter study, NFs based CHT and PCD were loaded with antiseptic agent (triclosan) for wound dressing application. We reported the role of cyclodextrins to improve the drug solubility, the sustained release of the drug and subsequently the prolongation of the antibacterial activity[40]. Following this work, the aim of the present study is to develop a covered stent coated with NFs based on CHT and β-cyclodextrin polymer (PCD). Simvastatin (SV), a lipid-lowering medication, was selected due to its pleiotropic effect. In particular, SV improves endothelial cell proliferation and reduces the proliferation of smooth muscle cells[41,42,43]. Recent studies suggest that statins protect endothelial cells by their action in the nitric oxide synthase system as well as by their antioxidant and anti-inflammatory effects. Firstly, the study of SV complexation with CD and the deposition of NFs onto the NiTiNOL stent was investigated through morphology and degradation studies. Then, the cytocompatibility of developed NFs was investigated, and finally, the *in vitro* release study of SV from NFs was assessed.

2. Materials and methods

2.1. Materials

Chitosan (CHT; Mw: 69 000 g/mol; deacetylation degree: 98 %, Beijing wisapple, China), polyethylene oxide (PEO; Mw: 900 000 g/mol, Sigma Aldrich, France), glacial acetic acid (AA, Sigma Aldrich, France), simvastatin (SV, Farmalabor, Italy), (2-hydroxypropyl)-β-cyclodextrin (HPβCD, Kleptose HP®, DS = 0.62 were kindly donated by Roquette (Lestrem, France)) and

synthesized HPβCD polymer Mw: 64 650 g/mol, weight CD content: 51 %w/w) were used for the inclusion complexation study and for the production of NFs. PolyHPβCD was synthesized according to the method reported by Martel *et al.*[44] from the reaction of esterification between HPβCD and citric acid acting as a crosslinking agent in the presence of sodium hypophosphite as catalyst. The water-soluble fractions of PCDs present a hyperbranched structure made of CD units (50 % in weight, determined by proton NMR) bridged by citrate crosslinks carrying free carboxylic groups providing their anionic character (4 mmol per gram, determined by acid-base titration).

Phosphate buffered saline (PBS, pH 7.4, Sigma Aldrich, France) and sodium dodecyl sulfate (SDS, Sigma Aldrich, France) were used for degradation study and release assays. All reagents were used as received from the manufacturer without further purification. Ultrapure water was used for all the experiments (18.2 MΩ, Purelab flex, ELGA, Veolia water aquadem, France).

2.2. Simvastatin / cyclodextrin interactions studies

2.2.1. Phase solubility diagram

The phase solubility diagram of SV in water in presence of native CDs and PCDs was obtained by the method reported by Higuchi and Connors[45]. Excess amount of SV (2 g/L) was added to aqueous solutions (pH = 6) containing various concentrations of CDs (0 to 100 g/L for HPβCD and polyHPβCD) in triplicate. The suspensions were placed in a rotative shaking incubator (Innova 40, Eppendorf, France) at room temperature (80 rpm for 24 hours). Then, the suspensions were filtered through a filtration membrane (cellulose acetate, pore diameter 0.45 µm, VWR^{TM} international) and analyzed by HPLC-UV (Shimadzu 2010C-HT) with a reverse column (Gemini C18 5 µm x 150 mm, Phenomenex, France) at 30°C. The mobile phase was composed of a 30:70 (v/v) mixture of potassium dihydrogen phosphate (KH_2PO_4, 3.5 g/L, pH 4.5, Sigma Aldrich, France) and acetonitrile (Sigma Aldrich, France). The flow rate was 0.8 mL/min and the injection volume 20 µL. SV was detected at 238 nm with a retention time of 4 min.

The phase solubility diagram was obtained by plotting the solubility of SV in mmol/L versus CD concentration in mmol/L. According to Brewster *et al.*[46], association constant (K_a) value of CD/SV inclusion complex was calculated from the slope of the linear part of the phase solubility diagrams using the following equation:

$$K_a = Slope / (S_0 * (1 - Slope))$$

Where S_0 is the intrinsic solubility of SV, i.e. the solubility in absence of cyclodextrin. *Slope* is the slope of the linear part of the phase–solubility profile.

The solubilizing power of CD was evaluated by the complexation efficiency (CE) parameter. CE is the complex to free CD concentrations ratio and was calculated from the slope of the phase solubility diagram:

$CE = S_0 * K_a = Slope / (1 – Slope)$

2.2.2. Preparation and physical characterization of CD/SV complexes

The inclusion complexes HPβCD/SV and PolyHPβCD/SV with a 1:1 stoichiometric ratio were prepared in water. The suspensions were placed in a rotative shaking incubator (Innova 40, Eppendorf, France) at room temperature (80 rpm, 24 hours, protected from light). The resulting solid complexes were put in the freezer at -20 °C for 24 hours and then freeze-dried (Alpha 1–2, Christ®, Germany) for 12 h (0.06 mBar, -53 °C) and stored at room temperature. Physical mixtures (PM) with the same ratio were prepared as control by mixing SV and CD or PCD in a mortar. Differential Scanning Calorimetry (DSC, TA Q100, TA Instruments, USA) studies were then carried out. 3 - 5 mg of inclusion complexes powders were placed in a sealed aluminum pan from -80 to 200 °C (10 °C/min) under nitrogen (50 mL/min). The structural characterization was analyzed by Powder X-Ray Diffraction (PXRD, PANalytical X'Pert pro MPD, Almelo, The Netherlands) equipped with a Cu X-ray tube (selected wavelength λCuKα = 1.54 Å) and the X'celerator detector. The samples were enclosed in a Lindemann glass capillary (diameter 0.7 mm) installed on a rotating sample holder. The measurements were performed in transmission mode with incident beam parabolic mirror.

2.3. Preparation and characterization of NFs covered stents

2.3.1. Preparation of electrospun solutions

HPβCD polymer (PCD: 0 and 3.3 % (w/v)) and SV (0.33 and 3.3 % (w/v)) were dissolved in 90 % (v/v) acetic acid solution in water and placed under stirring (350 rpm for 15 minutes) at room temperature. Then, CHT and PEO powder mixture (9:1) (w/w) were added to the solution and stirred at 450 rpm overnight. The electrospinning of CHT is limited by its polycationic nature in solution, and its rigid structure that prevents chains entanglements leading to jet break up. Therefore, PEO of high molecular weight is used to overcome these issues by forming hydrogen bonds with CHT polymeric chain segments, and supply chains entanglements[47].

The ratio of PCD-CHT in the mixture was based on our previous study[40]. In CHT/PCD/ SV0.33 NFs, SV was in default with regard to CD cavities (SV/CD = 0.75). Besides, the composition of CHT/PCD/SV3.3 NFs was defined to achieve the efficient therapeutic dose suggested in the literature[22]. As a consequence, SV was in large excess compared to CDs cavities in these NFs.

The composition of prepared electrospun solutions is detailed in table 1.

Table 1: Composition of electrospun solutions expressed in %w/v and theoretical composition of nanofibers expressed in %-wt estimated from the composition of the starting electrospun solutions

	Compound in acetic acid 90%(v/v)								**Viscosity (Pa.s)**
	CHT		**PEO**		**PCD**		**SV**		
	%w/v	**% wt**	**%w/v**	**% wt**	**% w/v**	**% wt**	**% w/v**	**% wt**	
CHT/SV0.33	2.97	82	0.33	9	0	0	0.33	9	0.61
CHT/PCD	2.97	45	0.33	5	3.3	50	0	0	1.59
CHT/PCD/SV0.33	2.97	43	0.33	4.7	3.3	47.6	0.33	4.7	1,59
CHT/PCD/SV3.3	2.97	30	0.33	3.4	3.3	33.3	3.3	33.3	1.65

2.3.2. Stent coating by electrospinning

Polymer solution was loaded into a 5 mL syringe placed onto a syringe pump (Fisher Scientific, France) operating with a flow rate of 0.3 mL/h and connected to a 21-gauge needle by the intermediate of polyethylene catheter (Inner diameter: 1 mm, Vygon, France). For preliminary tests, NFs were collected on an aluminum foil wrapping a stainless-steel cylindrical bar (∅ 5.5 mm) placed on a rotating mandrel (200 rpm) serving as collector. For the coating of stents with NFs, the aluminum foil was replaced by non-medicated NiTiNOL stents (6 x 40 mm) kindly provided by Cook® medical company (Zilver® Flex™, COOK® medical, France) threaded on the rotative mandrel. The distance between the needle and the collector was fixed at 20 cm and the applied voltage to 13 – 17 kV. Relative humidity and temperature were fixed at 28 ± 2 % and 22 ± 2 °C respectively. Three electrospinning durations (10, 20 and 30 minutes) were used in order to prepare stents with different coatings thicknesses. The NFs were finally heat-treated under vacuum at 120 °C for 4 hours in order to evaporate the residual solvent (Heraeus vacutherm, Thermoscientific, France).

2.3.3. NFs characterization

The individual morphology, the diameter of NFs and the thicknesses of NFs coatings on the stent were examined using scanning electron microscopy (SEM, Hitachi S-4700 SEM field emission GU, Japan) operating at an accelerating voltage of 5 kV and an emission current of 10 µA. All samples were sputtered beforehand with a thin layer of chrome before analysis. Attenuated Total Reflectance Fourier Transformed InfraRed (ATR-FTIR) spectra were recorded using a Spectrometer (Spectrum Two, Perkin Elmer, France) equipped with spectrum software from 4000 cm^{-1} to 650 cm^{-1} (scan number = 16) with a resolution of 4 cm^{-1}.

2.3.4. Stents crimping

The auto-expansible NiTiNOL stent used is supplied compressed in a delivery system composed of a 6 French catheter (2 mm).

Before electrospinning, the stent was released from its delivery system, and was threaded on the mandrel collector (diameter 5.5 mm) in its expanded form. After the NFs deposition, in order to ensure that covered stents are still compliant with the angioplasty surgical act, they must be re-conditioned inside the delivery catheter. Therefore, a crimper apparatus (HV200 transcatheter heart valve crimping tools, MSI, USA) (Figure 1) was used for constricting the stent and re-introduce it inside the catheter.

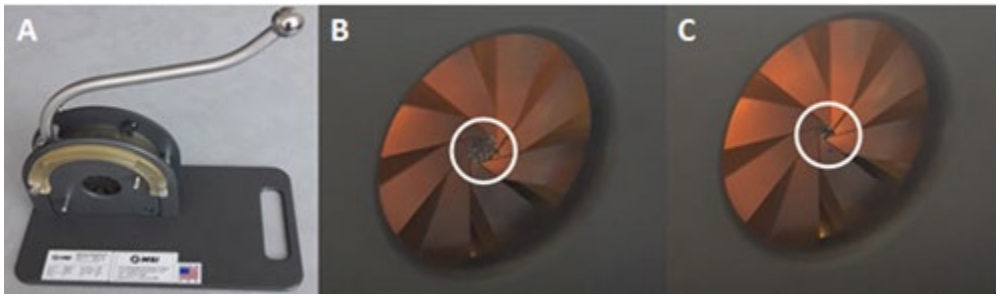

Figure 1: (A) Image of crimper apparatus, (B) and (C) stent crimping

2.3.5. NFs degradation studies

The degradation of NFs was followed by measuring the weight loss of NFs dipped in aqueous media. For this purpose, NFs (15 mg) covered stents were placed into 25 mL of phosphate buffered saline (PBS, pH 7.4) in a rotative shaking incubator (Thermoshake, Gerhardt France) under stirring (80 rpm) at 37 °C. The samples were removed after different time intervals (1, 4, 8, 12, 24, 48 and 72h), rinsed with distilled water, dried at 40 °C and finally weighed with a precision balance (KERN, Germany). The weight loss (WL) was calculated using the following equation:

$$WL\ (\%) = \frac{(\mathrm{W}_0 - W_t) * 100}{W_0}$$

Where W_0 is the initial dry weight (g) and W_t is the remaining dry weight (g) at specific sampling time.

2.3.6. Cytotoxicity tests

Biological tests were performed following the International and European standards (ISO 10993-5/EN 30993-5) with the human pulmonary microvascular endothelial cell line (HPMEC-ST1.6R). The cells were cultured in endothelial cell growth medium MV (PromoCell GmbH, Heidelberg, Germany) enriched with endothelial cell growth supplement (PromoCell GmbH, Heidelberg, Germany), streptomycin (0.1 g/L), and penicillin (100 IU/mL), at 37 °C in a CO_2 incubator (CB 150/APT line/ Binder, LabExchange, Paris, France) with 5% CO_2/ 95% atmosphere and 100% relative humidity.

Nanofibrous membrane disks (∅ 22 mm) were placed in 1 mL of complete culture medium (CCM) for 72 h at 37°C under agitation at 80 rpm (Innova40, New Brunswick Scientific, France). In parallel, 4.0×10^3 HPMEC cells per well were seeded in a 96-well tissue culture plate containing 100 µL of CCM per well. After 72 h, the extraction medium was collected and sterile filtered (0.2 µm, PB Acrodisc®; PALL, France). The culture medium was removed from the cells and 100 µL/well of the filtrated extraction medium or CCM (negative control), i.e. absence of cytotoxicity, were respectively added to the wells. After 24 h of incubation, the cell viability was measured by the AlamarBlue® assay (ThermoFisher Scientific, France). Briefly, extraction medium was removed from the cells and 200 µL/well of a 10% AlamarBlue® in CCM solution were added to the wells and placed, protected from light, in an incubator for 2 h. Then, 150 µL of the AlamarBlue® solution were recovered from each well and transferred into a flat bottom 96-well plate. Fluorescence was measured at an excitation wavelength of 530 nm and an emission wavelength of 590 nm, on a microplate fluorometer (TwinkleTMLB 970; Berthold Technologies GmbH & Co, Germany). The fluorescence readings were normalized relative to that of the negative controls. The experiments were performed in triplicate.

2.3.7. Simvastatin release study

In vitro SV release was performed in dynamic conditions using a fully automated flow through cell dissolution apparatus (CE 7 Smart dissolution apparatus, Sotax, Switzerland) operating in a closed loop configuration. SV loaded NFs stents (length: 4 cm, diameter: 6 mm) were placed

in flow cells (n=6). Drug release profiles were monitored in PBS/SDS (0.7 % v/v, 80 mL, pH 7.4) with a constant flow rate (35 mL/min) at 37°C. 100 µL of PBS/SDS were withdrawn at different time intervals and replaced with the same volume of fresh PBS/SDS up to 24 hours. The medium was analyzed by HPLC-UV using the same method described in the solubility study to determine the concentration of released SV. Each experiment was repeated 6 times.

2.3.8. Mechanism of drug release

Korsmeyer et *al.* derived a simple relationship which described drug release from polymeric system[48]. The mechanism of SV release (Fickian or non-Fickian) was studied using the first 60 % drug release data fitted in Korsmeyer-Peppas model:

$$\frac{M_t}{M_\infty} = \mathrm{k}t^n$$

Where: M_t / M_∞ is the fraction of drug released at time *t*, *k* is a constant characteristic of the drug-polymer system, and "*n"* is the diffusion exponent suggesting the nature of the release mechanism.

The "*n*" value is used to characterize different release mechanisms as given in the table 2:

Table 2: analysis of diffusional release mechanisms

Diffusion exponent (n)	Overall solute diffusion mechanism
0.45	Fickian diffusion
0.45 < n < 0.89	Anomalous (non-Fickian) diffusion
0.89	Case-II transport
n > 0.89	Super case-II transport

2.3.9. Statistical analysis

All data were expressed as the mean ± standard deviation (SD). Statistical test was performed by Statplus software (version Build 6.7.1.0/Core v6.2.02). Data were analyzed using one-way ANOVA and Tukey methods. The difference was regarded to be statistically significant for values of $p < 0.05$.

3. Results and discussion

3.1. CD-SV interaction study

The aqueous solubility of drugs is one of the key parameters in the bioavailability and the efficiency of medical treatments. SV is a lipophilic drug having a low solubility in water (0.26 mg/L, log p = 4.4, class II in the Biopharmaceutic classification System). The chemical structure of SV presents a lactone ring which can be hydrolyzed under acidic of alkaline conditions. Therefore, the solubility of SV can be influenced by the pH of the solution[49].

The enhancement of SV solubility in water using CDs was evaluated and presented in Figure 2. The phase solubility diagram of SV in the presence of HPβCD and polyHPβCD showed that solubility of SV increased linearly with the raising of CD concentration in the medium. The profiles of phase-solubility diagram are characteristic to A_L type solubility profiles following Higuchi and Connors classification suggesting a 1:1 mol/mol complex stoichiometry[45]. Interestingly, the calculated apparent stability constant $K_{1:1}$ of the HPβCD/SV complex is 1600 M^{-1} (CE = 0.003) while it increased up to 2500 M^{-1} (CE = 0.005) in case of polyHPβCD. It is noteworthy that the $K_{1:1}$ and CE values are low because of the extremely low solubility of SV in water (S_0 = $6.22.10^{-4}$ mmol/L at 20°C). Interestingly, considering the phase solubility diagram, it is clear that both HPβCD and polyHPβCD promote SV solubility in water. Moreover, slopes of both curves displayed in the phase solubility diagram and $K_{1:1}$ values show that polyHPβCD has a higher solubilizing effect on SV than non-polymerized HPβCD. In addition, it should be noted that no studies were reported on the enhancement of SV solubility using cyclodextrin polymers. These results can be explained by the cooperative action between neighboring CDs cavities in the hyperbranched macromolecular structure of these polymers and also to non-specific interactions between the polymeric network and the drug[50].

To support the hypothesis concerning the formation of inclusion complexes between CDs and SV, DSC and DRX studies were performed. Figure 3 presents the DSC curves of SV, CD/SV complexes and CD/SV PM. SV shows a sharp endothermic peak at 140 °C corresponding to the melting point (ΔH_f= 75 J/g), this peak is not observed in the HPβCD/SV and polyHPβCD/SV complexes. In addition, DSC curves of PM of SV with HPβCD and polyHPβCD showed the presence of an endothermic peak at 125 °C, which can be explained by the dissolution of SV in amorphous HPβCD and polyHPβCD [51]. According to these results, we can suppose that the amorphization of SV is due to its inclusion inside the CD cavity and in its dispersion in the polymer network of polyHPβCD.

Figure 3 presents the diffractograms of SV, CD/SV 1:1 complexes and PM. No signal corresponding to SV was observed in the diffractograms of HPβCD/SV and polyHPβCD/SV complexes, while some crystallographic peaks corresponding to SV are observed in the

HPβCD/SV and polyHPβCD/SV PM. These results support the hypothesis that HPβCD and polyHPβCD form an inclusion complex with SV. Finally, the complexation study confirmed the solubilizing properties of polyHPβCD (also named PCD thereafter) toward SV, and therefore justified its use in the formulation of the electrospun solutions developed hereafter, aiming to elaborate NFs for the prolonged delivery of SV.

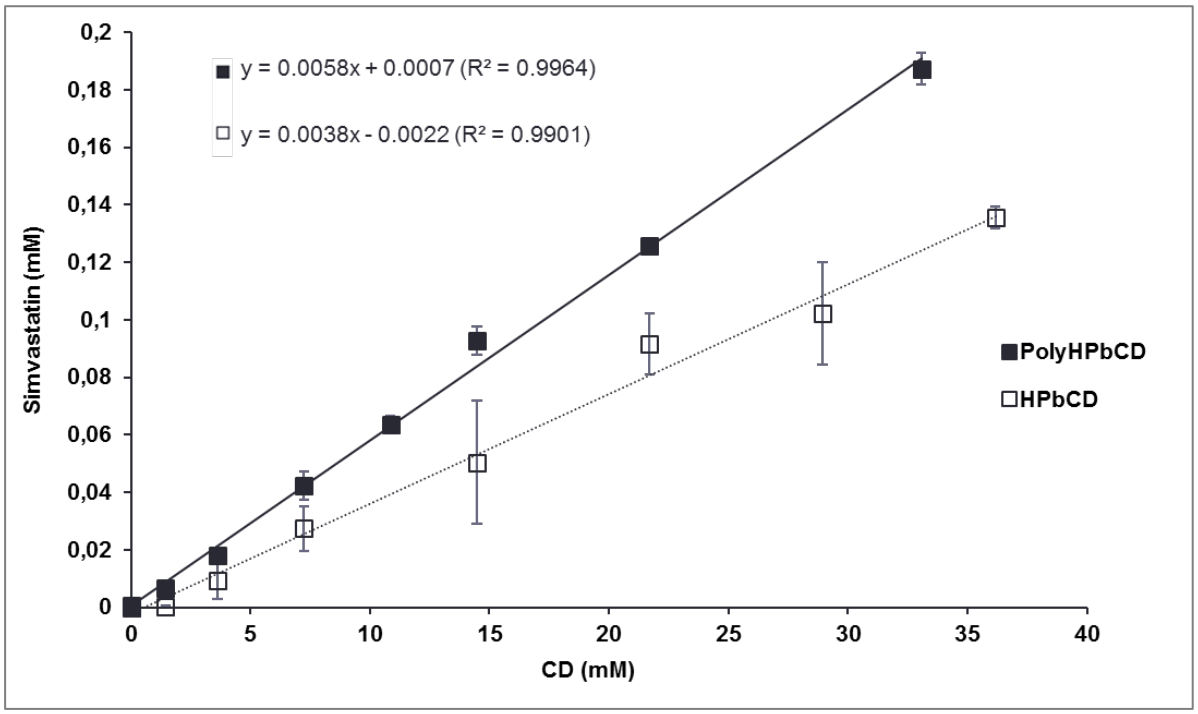

Figure 2: Phase solubility diagrams of SV in presence of HPβCD and polyHPβCD in water at room temperature after stirring (80 rpm, 24 hours)

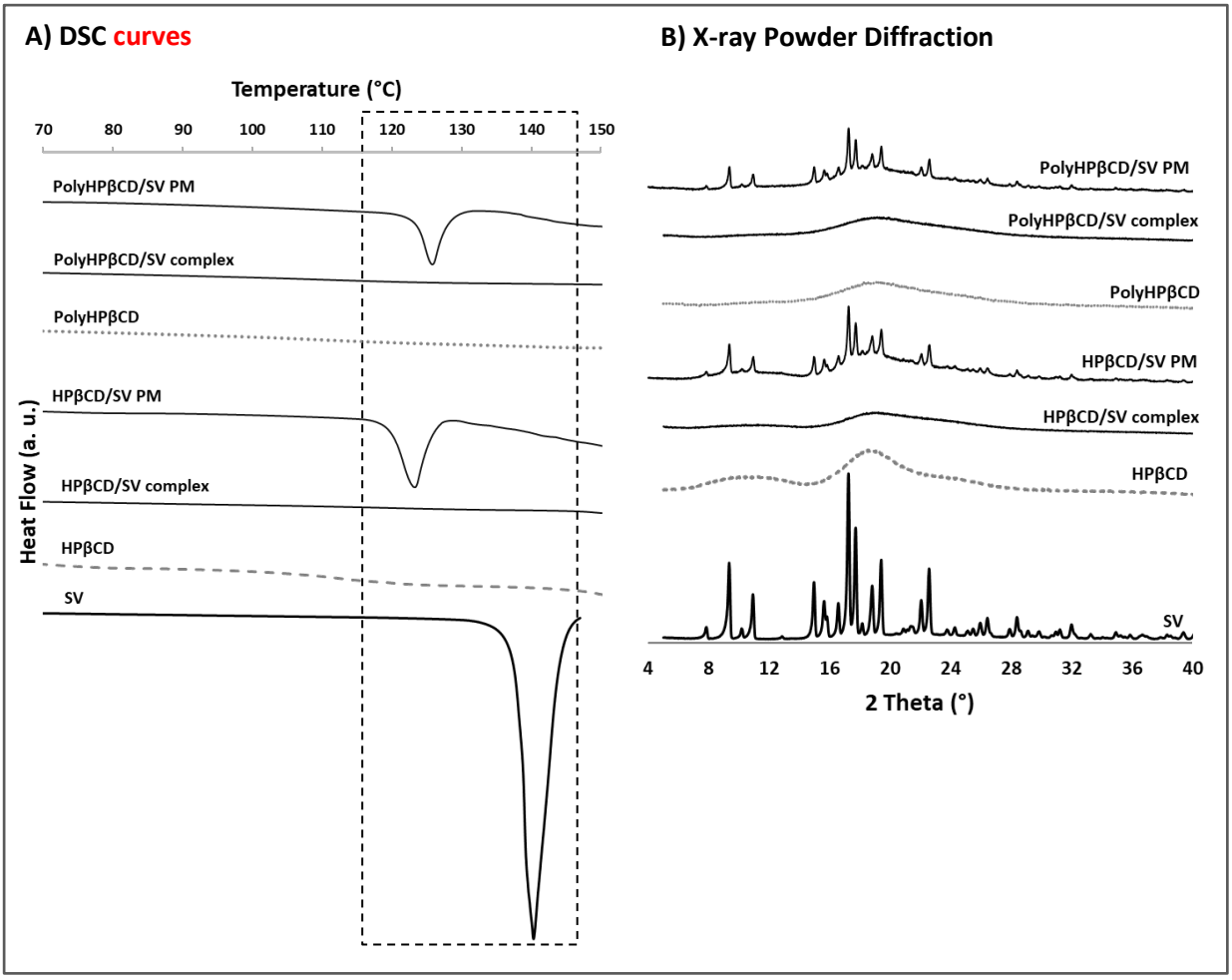

Figure 3: DSC curves (A) and X-ray Powder diffraction patterns (B) of SV, HPβCD, HPβCD/SV complex, HPβCD/SV physical mixture (PM), polyHPβCD, polyHPβCD/SV complex and polyHPβCD/SV physical mixture (PM) (1:1 molar ratio)

3.2. Morphology of NFs coated stents

The quantity of SV loaded on the stent depends on two main parameters: the SV dosage introduced in the electrospun solution on the one hand, and the duration of electrospinning on the other hand. The impact of these two parameters on the morphology, the thickness and the diameter of the NFs were studied. In a first approach, CHT/SV0.33, CHT/PCD/SV0.33 and CHT/PCD/SV3.3 solutions were electrospun onto the stent during 60 min (22 ± 2 °C, 28 ± 2 %RH). The obtained NFs were continuous, smooth and beadless with an average diameter of **270 ± 60 nm**, **500 ± 100 nm** and **520 ± 100 nm** respectively (figure 4). The presence of PCD drastically increased the diameter of NFs, which is explained by the increase of the viscosity of solutions (0.61 Pa.s for CHT/SV0.33 and 1.59 Pa.s for CHT/PCD/SV0.33 solutions). This viscosity increase is an evidence of electrostatic interactions between CHT and PCD leading to the formation of polyelectrolyte complexes[38]. Besides, no influence of SV concentration on NFs diameter could be observed.

As observed in figure 4, the electrospinning of CHT/PCD/SV0.33 mixture during 10, 30 and 60 minutes on stents resulted in the increase of the coatings thicknesses, respectively **125 ± 20 µm, 260 ± 40 µm** and **390 ± 70 µm**. Thereby, the electrospinning time allows to modulate the thickness of membranes and as a result, will allow to control the quantity of drug loaded on the stent[52].

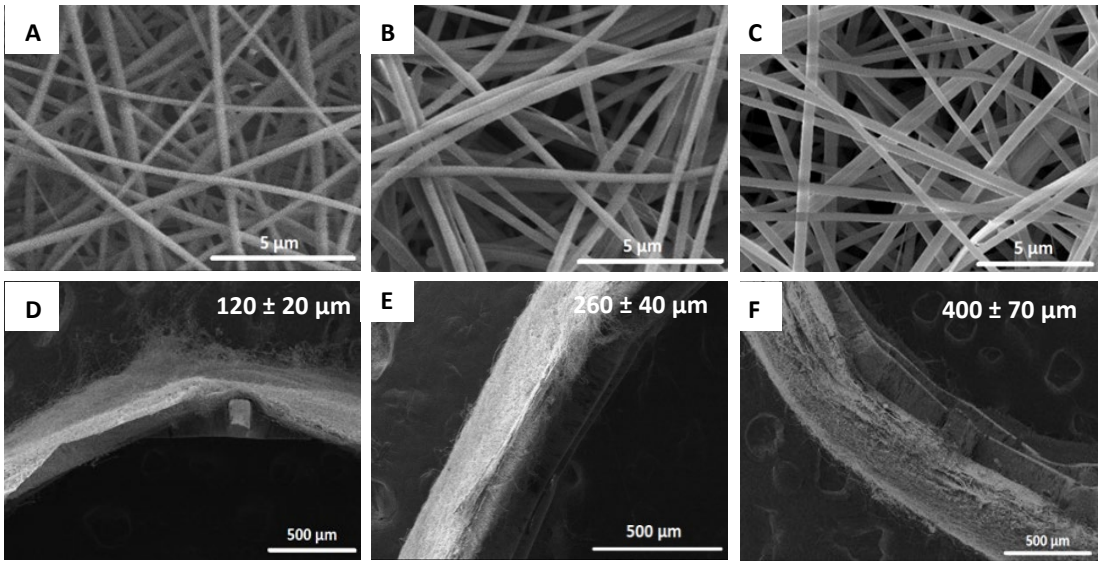

Figure 4: SEM micrographs of CHT/SV0.33 (A) CHT/PCD/SV0.33 (B) CHT/PCD/SV3.3 (C) NFs (60 min electrospinning, 22 ± 2°C, 28 ± 2 %RH) and thicknesses of CHT/PCD/SV0.33 coatings depending on the duration of electrospinning (D) 10 minutes, (E) 30 minutes, (F) 60 minutes

Self-expanding NiTiNOL stent is supplied constrained within 6-French delivery system corresponding to a catheter of 2 mm internal diameter. So, the self-expanding NiTiNOL stents were withdrawn from the sheath, placed on the 5.5 mm diameter rotative mandrel, and then covered by NFs by electrospinning. In an industrial context, the stents after their treatment by electrospinning should be conditioned in a delivery catheter. Therefore, this step was mimicked by using a specific "crimper" apparatus, used in industry for the construction of the stents prior to their insertion in the catheter.

As observed in figure 5b and 5c, the covered stent crimping operation caused a visible morphology change. However, no tear nor any degradation was observed on the membrane at the naked eye nor by using scanning electron microscopy (figures 5e-g) at low and high magnifications. Therefore, this investigation proved that our stents covered by electrospinning were compliant with the process of manufacturing the final medical device used by the surgeon in the operating theater.

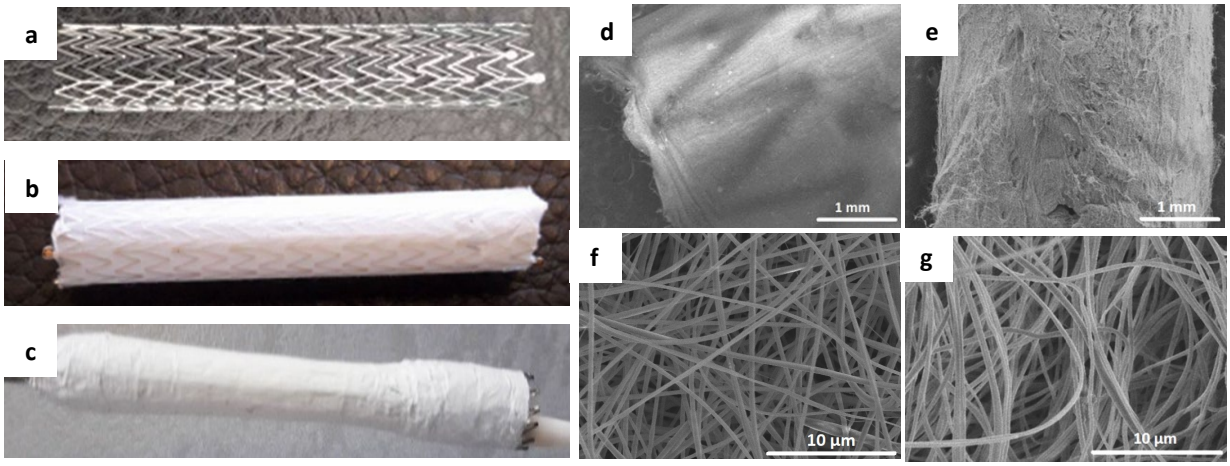

Figure 5: Macroscopic and microscopic images of Nitinol stent (a) covered with CHT/PCD/SV0.33 NFs before (b, d, f) and after crimping (c, e, g)

FTIR characterization was performed for detection of SV in the nanofibrous structure (figure 6). The spectrum of pure SV shows characteristic bands at 3547 cm^{-1} corresponding to alcoholic OH stretch vibration, 2955 and 2872 cm^{-1} which correspond to methyl and methylene C-H asymmetric and symmetric stretching vibration. The band at 1692 cm^{-1} is characteristic to lactone and ester groups (C=O) and the bands at 1260 cm^{-1} and 1158 cm^{-1} are attributed to lactone C-O-C bond stretching[53,54,55].

Figure 6 reports the superimposed spectra of CHT-PCD NFs and CHT-PCD NFs loaded with SV. The presence of SV in NFs is clearly visible in three places of the spectrum : i) around 2970 cm^{-1} corresponding to methyl and methylene C-H asymmetric and symmetric stretching

vibration in SV; ii) an increase of intensity of the band at 1700 cm^{-1} corresponding to the carbonyl groups of the lactone of SV and to the ester groups of PCD crosslinks and iii) the apparition of a peak situated at 1260 cm^{-1} and the increase of intensity of the band at 1150 cm^{-1} attributed to lactone -C-O-C stretching SV[53,54]. A detailed FTIR analysis of NFs composed of CHT, and PCD was previously reported[40]. In conclusion, the presence of SV in the NFs was detected through FTIR spectroscopy in highly loaded NFs. It is noteworthy that SV could not be detected in NFs prepared from solutions containing 0.33% of SV.

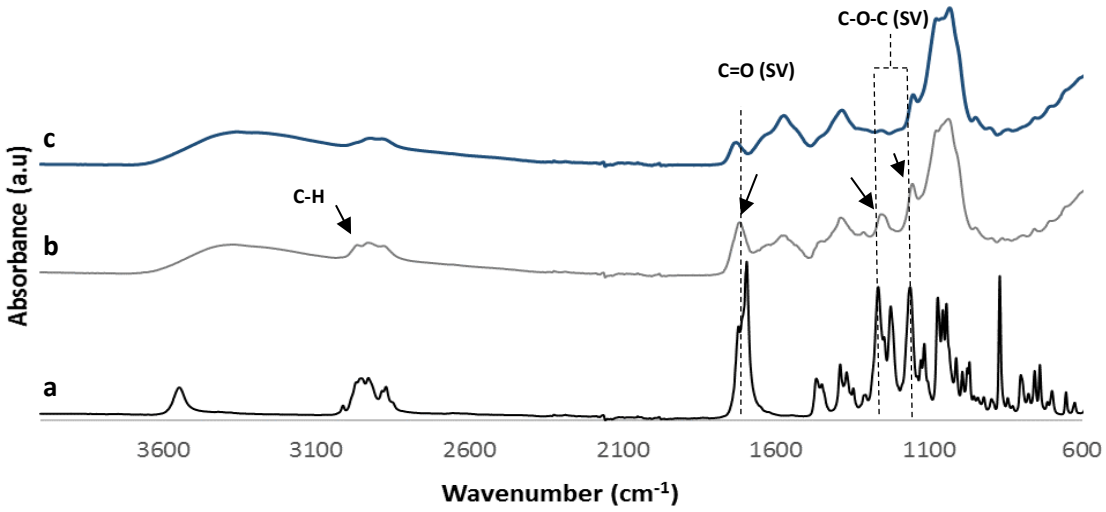

Figure 6: FTIR spectra of: a) pure simvastatin, b) NFs CHT/PCD/SV3.3, c) NFs CHT/PCD without simvastatin

3.3. NFs degradation study

Figure 7A shows the weight loss of CHT/SV0.33, CHT/PCD/SV0.33 and CHT/PCD/SV3.3 samples, post-heated at 120 °C for 4 hours, in PBS within 72 hours.

A rapid weight loss (13.7 ± 1.7 % in 8 hours) was observed with CHT/SV0.33 NFs due to the dissolution of highly soluble PEO in PBS (PEO represents 10 % weight in dry NFs). Then, after removal of PEO from the NFs, the NFs weight remained stable after 24 hours and up to 72 hours of degradation.

In the same way, a rapid and more important initial weight loss (36 ± 1.8 % in 8 hours) of CHT/PCD/SV0.33 NFs was observed due to the dissolution of both PEO and PCD, which are very soluble in aqueous medium (PCD and PEO represents 47.6 % and 4.7 % weight in dry

NFs, respectively). Besides, NFs loaded with 3.3 % w/v of SV (CHT/PCD/SV3.3) present the most important initial weight loss (45.4 ± 1.6 %) probably due to the dissolution of PEO, PCD and to the release of a few amount of SV from NFs matrix (representing 33% weight in dry NFs).

The SEM images of NFs after 8 hours and 72 hours of immersion in PBS are shown in figure 7B. CHT/SV0.3 were stable in PBS, a slight swelling was observed but the nanofibrous structure was conserved after 72 hours. Oppositely, an important swelling was noticed for CHT/PCD/SV0.33 and CHT/PCD/SV3.3 NFs after 8 hours. A progressive disappearance of nanofibrous structure was observed after 72 hours in aqueous media.

These results can be explained by the low stability of polyelectrolyte complexes in aqueous media, leading to the disintegration of the polymer matrix. This phenomenon was already observed in other systems based on CHT and PCD mixtures for the elaboration of spongy scaffolds[39] and layer-by-layer coatings[29]. We have reported that thermal post-treatments of these systems provoked the formation of amide links between PCD and CHT and increased their stability in water. In the present study, due to the melting point of SV at 140°C (the DSC curve of SV is presented in figure 3), NFs were post-heated at 120 °C for 4 hours. SEM study showed that these conditions could only partially ensure the NFs stabilization.

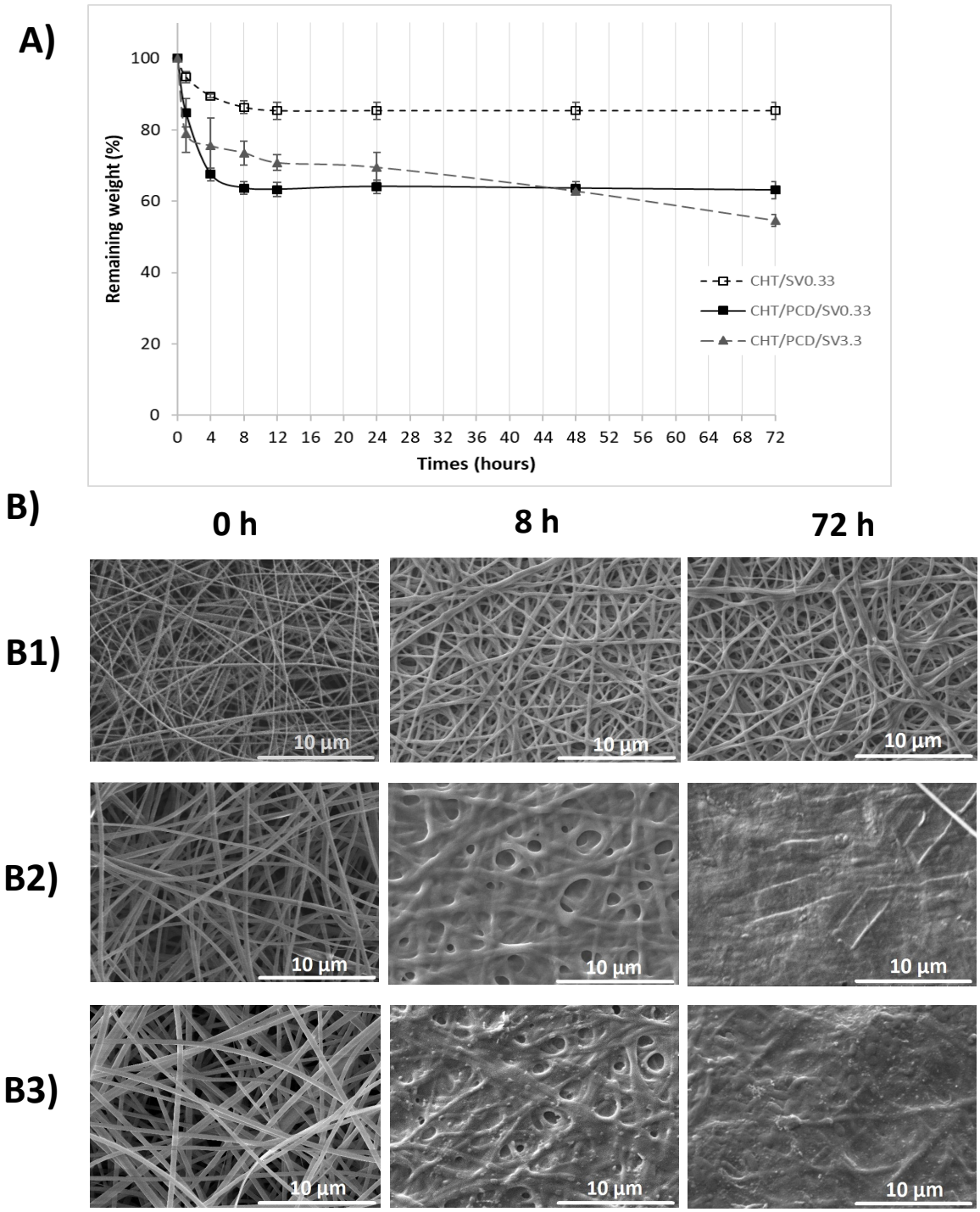

Figure 7: Evaluation of the degradation of CHT/SV0.33; CHT/PCD/SV0.33 and CHT/PCD/SV3.3 NFs by (A) weight loss measurement in PBS (pH 7.4, 37°C, 80 rpm) up to 72 hours and (B) SEM images of B1) CHT/SV0.33; B2) CHT/PCD/SV0.33 and B3) CHT/PCD/SV3.3 after immersion in PBS for 0; 8 and 72 hours.

3.4. Cell viability study

The NFs cytotoxicity was evaluated according to ISO/EN 10993-5 standard by the extraction method with Human Pulmonary Microvascular Endothelial Cells (HPMEC cells). The results are displayed in Figure 8.

Cytotoxicity evaluation of CHT/PCD NFs without SV directly after electrospinning exhibited no cell viability (2.4 ± 1.7 %) probably because of the presence of residual acetic acid in the NFs. An improved cytocompatibility (80.2 ± 3.3 %) has been obtained by rinsing these NFs subsequently 1 minute in a sodium bicarbonate ($NaHCO_3$, 4 g/L, Sigma Aldrich, France) solution and then 1 minute in 0.9 % saline (NaCl) solution to remove traces of acetic acid.

In the case of CHT/PCD/SV3.3 NFs, no cell viability has been observed even after the rinsing step with $NaHCO_3$ and NaCl (3.4 ± 0.2 % and 3.3 ± 0.2 % respectively). These results are presumably due to the toxicity against HPMEC of the SV liberated from the NFs in the culture medium. In order to investigate more specifically the intrinsic biological activity of SV, the cell viability of endothelial (HCAEC) and smooth muscle (HCSMC) cell lines has been studied versus SV concentration (figure S1 in supplementary data). Interestingly, the results clearly demonstrated a dose dependence effect, and moreover, HCAEC vitality was less affected than HCSMC in presence of SV. These results are in good agreement with the studies reported in the literature on the selective effect of SV on vascular cells[41,56]. Thereby, this confirms that SV is the good candidate to reach our objective as it presents the appropriate selectivity toward both types of cells present in the vessel wall.

Under the *in vitro* experimental conditions, the estimated amount of SV released in the extraction medium is higher than the cytocompatible concentration of SV. *In vivo* tests will be carried out to demonstrate the selective effect of SV loaded stent on the vascular cells.

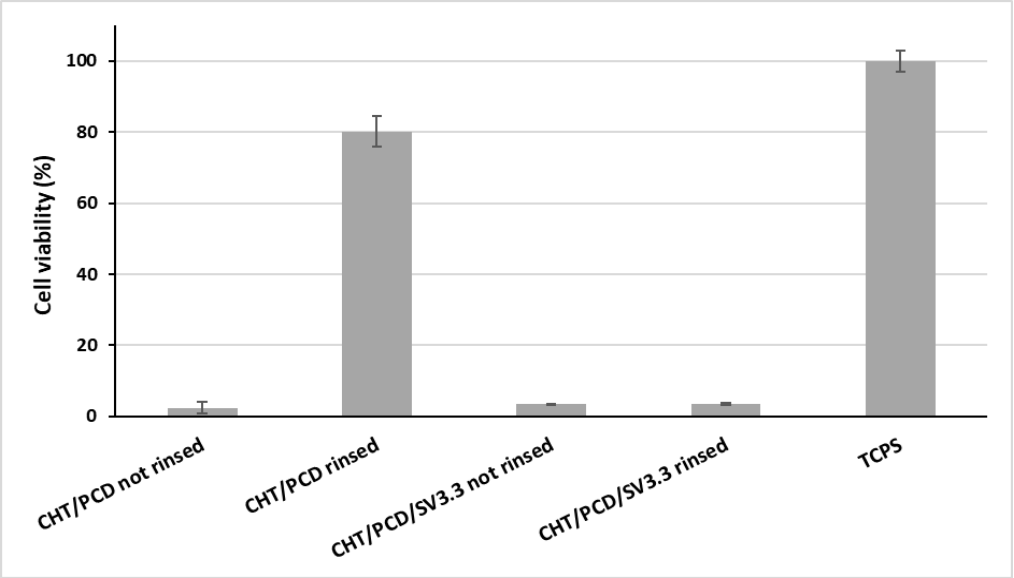

***Figure 8*:** Cell viability rate of HPMEC cells using the extraction method on CHT/PCD/SV3.3 and CHT/PCD electrospun NFs rinsed or not with $NaHCO_3$ (1 minute) and NaCl (1 minute)

3.5. Simvastatin release study

The release profiles of SV from NFs were investigated in dynamic conditions (35 mL/min) which correspond to the blood flow in coronary arteries[57]. The impact of electrospinning duration on the stent (i.e. coating thickness) and drug dosage in NFs on the release profiles were investigated.

a- Influence of electrospinning duration

Figure 9A displays the release kinetic profiles of SV from NFs obtained after 10, 30 and 60 minutes of electrospinning. The release of SV was rapid from NFs without PCD independently of the electrospinning time, with an important burst release effect. Indeed, more than 90% of SV loaded CHT/SV0.33 NFs were released within less than 30 minutes. Interestingly, the NFs containing CHT and PCD presented a prolonged release depending of the electrospinning time. 90% of total SV loading rates was released after 15, 120 and 300 minutes from stents coated during 10, 30, and 60 minutes.

This result can be explained by the formation of reversible inclusion complexes between CD and SV and by the entrapment of SV in PCD polymeric networks which allows a prolonged release of SV. Moreover, the total release time of SV is correlated with the electrospinning time and consequently with the thickness of the NFs coating.

The quantities of released SV increase with the raise of electrospinning durations and reach 0.4 $\mu g/mm^2$ for NFs containing PCD versus 0.21 $\mu g/mm^2$ for those without PCD for samples electrospun for 60 minutes (figure 9B). This significant difference ($p < 0.05$) is explained by the lower CHT/SV0.33 NFs weight deposited on the stent compared to CHT/PCD/SV0.33 NFs for similar electrospinning durations (figure 9C).

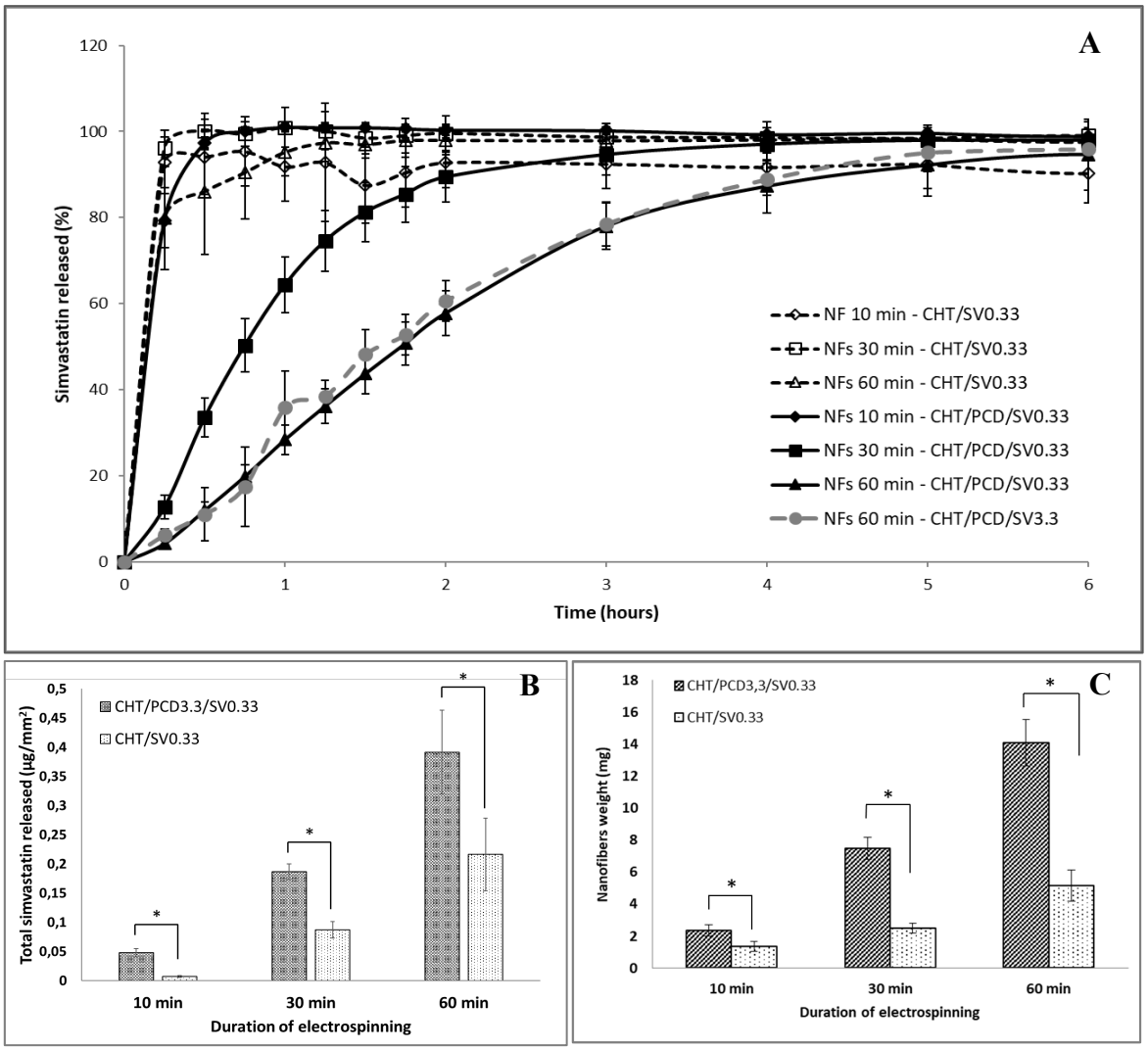

***Figure 9*: Release kinetics study of simvastatin in PBS/SDS0.7% pH =7.4 depending on the duration of electrospinning from NFs without and with PCD A) expressed in % of total SV initially loaded in NFs, B) expressed in µg of SV released per mm² of covered stent, C) NFs weight in mg deposited on the stent in mg versus the duration of electrospinning (*$p < 0.05$)**

b- Influence of simvastatin content in NFs

In our first approach, the amount of CD cavities available in the electrospun mixture was 1.5-fold higher than the amount of SV loaded in the NFs (0.33 %w/v). However, in practice, the SV dose loaded on the stent has to correspond to the efficient therapeutic dose, in other words, to the amount of drug that will induce the pleiotropic response *in vivo*. In the literature, Lee *et al.*[22] suggested that the therapeutic quantity of rosuvastatin loaded polylactic-co-glycolic acid NFs coated stent was comprised between 2 and 5 µg/mm^2. In this respect, the quantity of SV in the electrospun solution was increased from 0.33 %w/v to 3.3 %w/v in order to obtain NFs coatings able to deliver a higher and sufficient amount of SV. Consequently, the measured

delivered dose of SV by the covered stents increased from 0.39 ± 0.07 µg/mm^2 to 3 ± 0.12 µg/mm^2 (for an electrospinning time of 60 minutes).

Figure 9a shows that the release profiles of NFs issued from CHT/PCD/SV0.33 and CHT/PCD/SV3.3 formulations were superimposed (90% of SV released within 300 minutes).

Release kinetics data were treated using the Korsmeyer-Peppas mathematical model in order to determine the mechanism of SV release from the nanofibers. The n exposant values obtained for CHT/PCD/SV0.33 and CHT/PCD/SV3.3 NFs are 1.24 (R^2 = 0.99) and 1.16 (R^2 = 0.97) respectively. These values are superior to 0.89 indicating a non-Fickian diffusion (super case-II transport) suggesting an erosion/diffusion mechanism[48]. These results match with those of the degradation study where a progressive disappearance of nanofibrous structures has been observed after few hours of immersion in aqueous media.

The ideal drug kinetic release for DES is still unknown until now. It has been demonstrated by using drug eluting balloons, consisting on angiographic balloons coated with antirestenosis drug on their surface released locally into the vessel wall during balloon inflation, that a short time of contact (60 to 90 seconds) is sufficient to provide diffusion of lipophilic drugs through the vessel wall[58,59]. The potential advantages of drug eluting balloons are the rapid drug release providing the desired antiproliferative action with a little impact on long-term healing[60]. In our study, the same effect is expected by releasing SV in the few hours after implantation (6 hours according to *in vitro* studies). In the other hand, the hybrid DES developed in our study might have an anti-restenosis effect by the local delivery of statins which are associated with a pleiotropic effect reducing inflammatory response and improving endothelial function[41]. Accordingly, Jaschke *et al.* provided evidence that local application of cerivastatin on drug eluting stent can efficiently limit restenosis *in vivo* (rat model)[61]. On the other hand, the anti-restenosis activity of SV topically delivered from drug eluting stent has been previously reported by Zago *et al.* who tested a bare metal stent loaded with SV and showed that it was not related to a major adverse cardiac event. Nevertheless, it was associated with a high level of neointimal proliferation than expected probably because of the low dose of loaded SV [62].

Eventually, *in vivo* investigation will be mandatory to evaluate the diffusion of SV through the vessel wall and confirm that the 3.3 %w/v concentration of SV in the electrospun solution, and a surface concentration of 3 µg/mm² on the nanofibrous sheath of stent, will provide a stent that will display anti-restenosis activity.

4. Conclusion

Electrospinning was used for covering stents with nanofibers sheath for the elution of SV, used as pleiotropic agent in restenosis prevention. NFs were based on CHT and PCD polyelectrolyte complex. PolyHPβCD through inclusion complex formation enhanced the solubility of lipophilic SV in aqueous solutions and prolonged the release of SV from the nanofibrous electrospun nanoweb. SV loading rates on the stent could be controlled by SV concentration in the electrospun CHT/PCD solutions (0.33 and 3.3 %w/v) on the one hand, and by the coating thickness and electrospinning time on the other hand. The "crimper" test showed that the covered self-expanding stent could be inserted inside the delivery catheter without damage of NFs sheath, which is an important point to consider for industrial process. The kinetic release study demonstrated that the extension of the release time of SV depended on the duration of electrospinning and on the presence of PCD in NFs matrix. Thermal treatment prevented rapid degradation of NFs and appropriate rinsing step provided them acceptable cytocompatibility. The advantage of NFs coated stent is that NFs sheath may be potentially loaded with higher doses of drugs compared to the drug reservoir capacity of classical coated active stents which is limited by the reduced area of stent strut. The next step of our study will concern *in vivo* tests to investigate in depth the influence of the SV dose loaded on the stent, and to determine its optimal value in the reduction of neointimal hyperplasia.

Acknowledgments

This study was supported by the Interreg 2 Seas program 2014-2020 co-funded by the European Regional Development Fund under subsidy contract 2S01-059_IMODE, the University of Lille and the Chevreul Institute (FR2638). The authors would like to thank COOK® medical company for the provided stents, and Florence Danède for X-ray Powder Diffraction analysis.

References

(1) Roth, G. A.; Johnson, C.; Abajobir, A.; Abd-Allah, F.; Abera, S. F.; Abyu, G.; Ahmed, M.; Aksut, B.; Alam, T.; Alam, K.; et al. Global, Regional, and National Burden of Cardiovascular Diseases for 10 Causes, 1990 to 2015. *J. Am. Coll. Cardiol.* **2017**, *70* (1), 1–25. https://doi.org/10.1016/j.jacc.2017.04.052.

(2) Lusis, A. J. Atherosclerosis. *Nature* **2000**, *407*, 233–241. https://doi.org/10.1038/35025203.

(3) Cruden, N.; Wilson. Advances in Coronary Stent Technology: Current Expectations and New Developments. *Res. Rep. Clin. Cardiol.* **2013**, 85. https://doi.org/10.2147/RRCC.S34408.

(4) Bennett, M. R.; O'Sullivan, M. Mechanisms of Angioplasty and Stent Restenosis: Implications for Design of Rational Therapy. *Pharmacol. Ther.* **2001**, *91* (2), 149–166. https://doi.org/10.1016/S0163-7258(01)00153-X.

(5) Stone, G. W.; Ellis, S. G.; Cannon, L.; Mann, J. T.; Greenberg, J. D.; Spriggs, D.; O'Shaughnessy, C. D.; DeMaio, S.; Hall, P.; Popma, J. J.; et al. Comparison of a Polymer-Based Paclitaxel-Eluting

Stent With a Bare Metal Stent in Patients With Complex Coronary Artery Disease: A Randomized Controlled Trial. *JAMA* **2005**, *294* (10), 1215–1223. https://doi.org/10.1001/jama.294.10.1215.

(6) Morice, M.-C.; Serruys, P. W.; Sousa, J. E.; Fajadet, J.; Ban Hayashi, E.; Perin, M.; Colombo, A.; Schuler, G.; Barragan, P.; Guagliumi, G.; et al. A Randomized Comparison of a Sirolimus-Eluting Stent with a Standard Stent for Coronary Revascularization https://www.nejm.org/doi/10.1056/NEJMoa012843?url_ver=Z39.88-2003&rfr_id=ori%3Arid%3Acrossref.org&rfr_dat=cr_pub%3Dwww.ncbi.nlm.nih.gov (accessed May 27, 2019). https://doi.org/10.1056/NEJMoa012843.

(7) Blanchemain, N.; Sobocinski, J.; Maurel-Desanlis, B.; Hertault, A.; Haulon, S. Stent Surface Modification: Where Are We Today. In *Current Challenges in vascular Biomaterials*; ESVB; 2015; Vol. 26, pp 253–266.

(8) Seo, J.; Lee, J.; Na, K. Polymeric Materials for Drug Release System in Drug Eluting Stents. *J. Pharm. Investig.* **2016**, *46* (4), 317–324. https://doi.org/10.1007/s40005-016-0251-2.

(9) Acharya, G.; Park, K. Mechanisms of Controlled Drug Release from Drug-Eluting Stents. *Adv. Drug Deliv. Rev.* **2006**, *58* (3), 387–401. https://doi.org/10.1016/j.addr.2006.01.016.

(10) Windecker, S.; Serruys, P. W.; Wandel, S.; Buszman, P.; Trznadel, S.; Linke, A.; Lenk, K.; Ischinger, T.; Klauss, V.; Eberli, F.; et al. Biolimus-Eluting Stent with Biodegradable Polymer versus Sirolimus-Eluting Stent with Durable Polymer for Coronary Revascularisation (LEADERS): A Randomised Non-Inferiority Trial. *The Lancet* **2008**, *372* (9644), 1163–1173. https://doi.org/10.1016/S0140-6736(08)61244-1.

(11) Oh, B.; Lee, C. H. Advanced Cardiovascular Stent Coated with Nanofiber. *Mol. Pharm.* **2013**, *10* (12), 4432–4442. https://doi.org/10.1021/mp400231p.

(12) Huang, Y.; Venkatraman, S. S.; Boey, F. Y. C.; Lahti, E. M.; Umashankar, P. R.; Mohanty, M.; Arumugam, S.; Khanolkar, L.; Vaishnav, S. In Vitro and in Vivo Performance of a Dual Drug-Eluting Stent (DDES). *Biomaterials* **2010**, *31* (15), 4382–4391. https://doi.org/10.1016/j.biomaterials.2010.01.147.

(13) Chen, M.-C.; Liang, H.-F.; Chiu, Y.-L.; Chang, Y.; Wei, H.-J.; Sung, H.-W. A Novel Drug-Eluting Stent Spray-Coated with Multi-Layers of Collagen and Sirolimus. *J. Controlled Release* **2005**, *108* (1), 178–189. https://doi.org/10.1016/j.jconrel.2005.07.022.

(14) Bhambri, P.; Sarvi, A.; Wong, J. H.; Sundararaj, U.; Mitha, A. P. Verapamil Eluting Stents as a Possible Treatment for Vasospasm after Subarachnoid Hemorrhage. *J. NeuroInterventional Surg.* **2017**, *9* (9), 875–879. https://doi.org/10.1136/neurintsurg-2016-012521.

(15) Qi, H.; Ye, Z.; Ren, H.; Chen, N.; Zeng, Q.; Wu, X.; Lu, T. Bioactivity Assessment of PLLA/PCL/HAP Electrospun Nanofibrous Scaffolds for Bone Tissue Engineering. *Life Sci.* **2016**, *148*, 139–144. https://doi.org/10.1016/j.lfs.2016.02.040.

(16) Montero, R. B.; Vial, X.; Nguyen, D. T.; Farhand, S.; Reardon, M.; Pham, S. M.; Tsechpenakis, G.; Andreopoulos, F. M. BFGF-Containing Electrospun Gelatin Scaffolds with Controlled Nano-Architectural Features for Directed Angiogenesis. *Acta Biomater.* **2012**, *8* (5), 1778–1791. https://doi.org/10.1016/j.actbio.2011.12.008.

(17) Chou, S.-F.; Carson, D.; Woodrow, K. A. Current Strategies for Sustaining Drug Release from Electrospun Nanofibers. *J. Controlled Release* **2015**, *220*, 584–591. https://doi.org/10.1016/j.jconrel.2015.09.008.

(18) Kajdič, S.; Planinšek, O.; Gašperlin, M.; Kocbek, P. Electrospun Nanofibers for Customized Drug-Delivery Systems. *J. Drug Deliv. Sci. Technol.* **2019**, *51*, 672–681. https://doi.org/10.1016/j.jddst.2019.03.038.

(19) Cheng, H.; Yang, X.; Che, X.; Yang, M.; Zhai, G. Biomedical Application and Controlled Drug Release of Electrospun Fibrous Materials. *Mater. Sci. Eng. C* **2018**, *90*, 750–763. https://doi.org/10.1016/j.msec.2018.05.007.

(20) Oh, B.; Lee, C. H. Nanofiber for Cardiovascular Tissue Engineering. *Expert Opin. Drug Deliv.* **2013**, *10* (11), 1565–1582. https://doi.org/10.1517/17425247.2013.830608.

(21) Hu, X.; Liu, S.; Zhou, G.; Huang, Y.; Xie, Z.; Jing, X. Electrospinning of Polymeric Nanofibers for Drug Delivery Applications. *J. Controlled Release* **2014**, *185*, 12–21. https://doi.org/10.1016/j.jconrel.2014.04.018.

(22) Lee, C.-H.; Chang, S.-H.; Lin, Y.-H.; Liu, S.-J.; Wang, C.-J.; Hsu, M.-Y.; Hung, K.-C.; Yeh, Y.-H.; Chen, W.-J.; Hsieh, I.-C.; et al. Acceleration of Re-Endothelialization and Inhibition of Neointimal Formation Using Hybrid Biodegradable Nanofibrous Rosuvastatin-Loaded Stents. *Biomaterials* **2014**, *35* (15), 4417–4427. https://doi.org/10.1016/j.biomaterials.2014.02.017.

(23) Tang, J.; Liu, Y.; Zhu, B.; Su, Y.; Zhu, X. Preparation of Paclitaxel/Chitosan Co-Assembled Core-Shell Nanofibers for Drug-Eluting Stent. *Appl. Surf. Sci.* **2017**, *393*, 299–308. https://doi.org/10.1016/j.apsusc.2016.10.015.

(24) Karuppuswamy, P.; Reddy Venugopal, J.; Navaneethan, B.; Luwang Laiva, A.; Ramakrishna, S. Polycaprolactone Nanofibers for the Controlled Release of Tetracycline Hydrochloride. *Mater. Lett.* **2015**, *141*, 180–186. https://doi.org/10.1016/j.matlet.2014.11.044.

(25) Son, Y. J.; Kim, H. S.; Choi, D. H.; Yoo, H. S. Multilayered Electrospun Fibrous Meshes for Restenosis-Suppressing Metallic Stents. *J. Biomed. Mater. Res. B Appl. Biomater.* **2015**, n/a-n/a. https://doi.org/10.1002/jbm.b.33583.

(26) Aytac, Z.; Sen, H. S.; Durgun, E.; Uyar, T. Sulfisoxazole/Cyclodextrin Inclusion Complex Incorporated in Electrospun Hydroxypropyl Cellulose Nanofibers as Drug Delivery System. *Colloids Surf. B Biointerfaces* **2015**, *128*, 331–338. https://doi.org/10.1016/j.colsurfb.2015.02.019.

(27) Loftsson, T.; Jarho, P.; Másson, M.; Järvinen, T. Cyclodextrins in Drug Delivery. *Expert Opin. Drug Deliv.* **2005**, *2* (2), 335–351. https://doi.org/10.1517/17425247.2.1.335.

(28) Garcia-Fernandez, M. J.; Tabary, N.; Chai, F.; Cazaux, F.; Blanchemain, N.; Flament, M.-P.; Martel, B. New Multifunctional Pharmaceutical Excipient in Tablet Formulation Based on Citric Acid-Cyclodextrin Polymer. *Int. J. Pharm.* **2016**, *511* (2), 913–920. https://doi.org/10.1016/j.ijpharm.2016.07.059.

(29) Aubert-Viard, F.; Mogrovejo-Valdivia, A.; Tabary, N.; Maton, M.; Chai, F.; Neut, C.; Martel, B.; Blanchemain, N. Evaluation of Antibacterial Textile Covered by Layer-by-Layer Coating and Loaded with Chlorhexidine for Wound Dressing Application. *Mater. Sci. Eng. C* **2019**, *100*, 554–563. https://doi.org/10.1016/j.msec.2019.03.044.

(30) García-Fernández, M. J.; Tabary, N.; Martel, B.; Cazaux, F.; Oliva, A.; Taboada, P.; Concheiro, A.; Alvarez-Lorenzo, C. Poly-(Cyclo)Dextrins as Ethoxzolamide Carriers in Ophthalmic Solutions and in Contact Lenses. *Carbohydr. Polym.* **2013**, *98* (2), 1343–1352. https://doi.org/10.1016/j.carbpol.2013.08.003.

(31) Sobocinski, J.; Laure, W.; Taha, M.; Courcot, E.; Chai, F.; Simon, N.; Addad, A.; Martel, B.; Haulon, S.; Woisel, P.; et al. Mussel Inspired Coating of a Biocompatible Cyclodextrin Based Polymer onto CoCr Vascular Stents. *ACS Appl. Mater. Interfaces* **2014**, *6* (5), 3575–3586. https://doi.org/10.1021/am405774v.

(32) Tapia, C.; Escobar, Z.; Costa, E.; Sapag-Hagar, J.; Valenzuela, F.; Basualto, C.; Nella Gai, M.; Yazdani-Pedram, M. Comparative Studies on Polyelectrolyte Complexes and Mixtures of Chitosan–Alginate and Chitosan–Carrageenan as Prolonged Diltiazem Clorhydrate Release Systems. *Eur. J. Pharm. Biopharm.* **2004**, *57* (1), 65–75. https://doi.org/10.1016/S0939-6411(03)00153-X.

(33) Thierry, B.; Winnik, F. M.; Merhi, Y.; Silver, J.; Tabrizian, M. Bioactive Coatings of Endovascular Stents Based on Polyelectrolyte Multilayers. *Biomacromolecules* **2003**, *4* (6), 1564–1571. https://doi.org/10.1021/bm0341834.

(34) Meng, S.; Liu, Z.; Shen, L.; Guo, Z.; Chou, L. L.; Zhong, W.; Du, Q.; Ge, J. The Effect of a Layer-by-Layer Chitosan–Heparin Coating on the Endothelialization and Coagulation Properties of a Coronary Stent System. *Biomaterials* **2009**, *30* (12), 2276–2283. https://doi.org/10.1016/j.biomaterials.2008.12.075.

(35) Pérez-Anes, A.; Gargouri, M.; Laure, W.; Van Den Berghe, H.; Courcot, E.; Sobocinski, J.; Tabary, N.; Chai, F.; Blach, J.-F.; Addad, A.; et al. Bioinspired Titanium Drug Eluting Platforms Based on

a Poly-β-Cyclodextrin–Chitosan Layer-by-Layer Self-Assembly Targeting Infections. *ACS Appl. Mater. Interfaces* **2015**, *7* (23), 12882–12893. https://doi.org/10.1021/acsami.5b02402.

(36) Martin, A.; Tabary, N.; Leclercq, L.; Junthip, J.; Degoutin, S.; Aubert-Viard, F.; Cazaux, F.; Lyskawa, J.; Janus, L.; Bria, M.; et al. Multilayered Textile Coating Based on a β-Cyclodextrin Polyelectrolyte for the Controlled Release of Drugs. *Carbohydr. Polym.* **2013**, *93* (2), 718–730. https://doi.org/10.1016/j.carbpol.2012.12.055.

(37) Mogrovejo-Valdivia, A.; Rahmouni, O.; Tabary, N.; Maton, M.; Neut, C.; Martel, B.; Blanchemain, N. In Vitro Evaluation of Drug Release and Antibacterial Activity of a Silver-Loaded Wound Dressing Coated with a Multilayer System. *Int. J. Pharm.* **2019**, *556*, 301–310. https://doi.org/10.1016/j.ijpharm.2018.12.018.

(38) Palomino-Durand, C.; Lopez, M.; Cazaux, F.; Martel, B.; Blanchemain, N.; Chai, F. Influence of the Soluble–Insoluble Ratios of Cyclodextrins Polymers on the Viscoelastic Properties of Injectable Chitosan–Based Hydrogels for Biomedical Application. *Polymers* **2019**, *11* (2), 214. https://doi.org/10.3390/polym11020214.

(39) Flores, C.; Lopez, M.; Tabary, N.; Neut, C.; Chai, F.; Betbeder, D.; Herkt, C.; Cazaux, F.; Gaucher, V.; Martel, B.; et al. Preparation and Characterization of Novel Chitosan and β-Cyclodextrin Polymer Sponges for Wound Dressing Applications. *Carbohydr. Polym.* **2017**, *173*, 535–546. https://doi.org/10.1016/j.carbpol.2017.06.026.

(40) Ouerghemmi, S.; Degoutin, S.; Tabary, N.; Cazaux, F.; Maton, M.; Gaucher, V.; Janus, L.; Neut, C.; Chai, F.; Blanchemain, N.; et al. Triclosan Loaded Electrospun Nanofibers Based on a Cyclodextrin Polymer and Chitosan Polyelectrolyte Complex. *Int. J. Pharm.* **2016**, *513* (1), 483–495. https://doi.org/10.1016/j.ijpharm.2016.09.060.

(41) Sadowitz, B.; Maier, K. G.; Gahtan, V. Basic Science Review: Statin Therapy-Part I: The Pleiotropic Effects of Statins in Cardiovascular Disease. *Vasc. Endovascular Surg.* **2010**, *44* (4), 241–251. https://doi.org/10.1177/1538574410362922.

(42) Endres, M. Statins: Potential New Indications in Inflammatory Conditions. *Atheroscler. Suppl.* **2006**, *7* (1), 31–35. https://doi.org/10.1016/j.atherosclerosissup.2006.01.005.

(43) Gelosa, P.; Cimino, M.; Pignieri, A.; Tremoli, E.; Guerrini, U.; Sironi, L. The Role of HMG-CoA Reductase Inhibition in Endothelial Dysfunction and Inflammation. *Vasc. Health Risk Manag.* **2007**, *3* (5), 567–577.

(44) Martel, B.; Ruffin, D.; Weltrowski, M.; Lekchiri, Y.; Morcellet, M. Water-Soluble Polymers and Gels from the Polycondensation between Cyclodextrins and Poly(Carboxylic Acid)s: A Study of the Preparation Parameters. *J. Appl. Polym. Sci.* **2005**, *97* (2), 433–442. https://doi.org/10.1002/app.21391.

(45) Higuchi, T.; Connors, K. A. Phase Solubility Techniques. *Advances in Analytical Chemistry and Instrumentation*. 1965, pp 117–212.

(46) Brewster, M. E.; Loftsson, T. Cyclodextrins as Pharmaceutical Solubilizers. *Adv. Drug Deliv. Rev.* **2007**, *59* (7), 645–666. https://doi.org/10.1016/j.addr.2007.05.012.

(47) Pakravan, M.; Heuzey, M.-C.; Ajji, A. A Fundamental Study of Chitosan/PEO Electrospinning. *Polymer* **2011**, *52* (21), 4813–4824. https://doi.org/10.1016/j.polymer.2011.08.034.

(48) Korsmeyer, R. W.; Gurny, R.; Doelker, E.; Buri, P.; Peppas, N. A. Mechanisms of Solute Release from Porous Hydrophilic Polymers. *Int. J. Pharm.* **1983**, *15* (1), 25–35. https://doi.org/10.1016/0378-5173(83)90064-9.

(49) Ellison, D. K.; Moore, W. D.; Petts, C. R. Simvastatin. In *Analytical Profiles of Drug Substances and Excipients*; Brittain, H. G., Ed.; Academic Press, 1993; Vol. 22, pp 359–388. https://doi.org/10.1016/S0099-5428(08)60246-4.

(50) Danel, C.; Azaroual, N.; Chavaria, C.; Odou, P.; Martel, B.; Vaccher, C. Comparative Study of the Complex Forming Ability and Enantioselectivity of Cyclodextrin Polymers by CE and 1H NMR. *Carbohydr. Polym.* **2013**, *92* (2), 2282–2292. https://doi.org/10.1016/j.carbpol.2012.11.095.

(51) Mahieu, A.; Willart, J.-F.; Dudognon, E.; Danède, F.; Descamps, M. A New Protocol To Determine the Solubility of Drugs into Polymer Matrixes. *Mol. Pharm.* **2013**, *10* (2), 560–566. https://doi.org/10.1021/mp3002254.

(52) Bhambri, P.; Sarvi, A.; Wong, J. H.; Sundararaj, U.; Mitha, A. P. Verapamil Eluting Stents as a Possible Treatment for Vasospasm after Subarachnoid Hemorrhage. *J. NeuroInterventional Surg.* **2017**, *9* (9), 875–879. https://doi.org/10.1136/neurintsurg-2016-012521.

(53) Jun, S. W.; Kim, M.-S.; Kim, J.-S.; Park, H. J.; Lee, S.; Woo, J.-S.; Hwang, S.-J. Preparation and Characterization of Simvastatin/Hydroxypropyl-β-Cyclodextrin Inclusion Complex Using Supercritical Antisolvent (SAS) Process. *Eur. J. Pharm. Biopharm.* **2007**, *66* (3), 413–421. https://doi.org/10.1016/j.ejpb.2006.11.013.

(54) Nath, S. D.; Son, S.; Sadiasa, A.; Min, Y. K.; Lee, B. T. Preparation and Characterization of PLGA Microspheres by the Electrospraying Method for Delivering Simvastatin for Bone Regeneration. *Int. J. Pharm.* **2013**, *443* (1), 87–94. https://doi.org/10.1016/j.ijpharm.2012.12.037.

(55) Mandal, D.; Ojha, P. K.; Nandy, B. C.; Kanta, L. Effect of Carriers on Solid Dispersions of Simvastatin (Sim): Physico- Chemical Characterizations and Dissolution Studies. **2010**, 10.

(56) Bellosta, S.; Bernini, F.; Ferri, N.; Quarato, P.; Canavesi, M.; Arnaboldi, L.; Fumagalli, R.; Paoletti, R.; Corsini, A. Direct Vascular Effects of HMG-CoA Reductase Inhibitors. *Atherosclerosis* **1998**, *137*, S101–S109. https://doi.org/10.1016/S0021-9150(97)00319-5.

(57) Seidlitz, A.; Nagel, S.; Semmling, B.; Grabow, N.; Martin, H.; Senz, V.; Harder, C.; Sternberg, K.; Schmitz, K.-P.; Kroemer, H. K.; et al. Examination of Drug Release and Distribution from Drug-Eluting Stents with a Vessel-Simulating Flow-through Cell. *Eur. J. Pharm. Biopharm.* **2011**, *78* (1), 36–48. https://doi.org/10.1016/j.ejpb.2010.12.021.

(58) Tesfamariam, B. Local Arterial Wall Drug Delivery Using Balloon Catheter System. *J. Controlled Release* **2016**, *238*, 149–156. https://doi.org/10.1016/j.jconrel.2016.07.041.

(59) Meneguz-Moreno, R. A.; Ribamar Costa, J.; Abizaid, A. Drug-Coated Balloons: Hope or Hot Air: Update on the Role of Coronary DCB. *Curr. Cardiol. Rep.* **2018**, *20* (10), 100. https://doi.org/10.1007/s11886-018-1025-4.

(60) Waksman Ron; Pakala Rajbabu. Drug-Eluting Balloon. *Circ. Cardiovasc. Interv.* **2009**, *2* (4), 352–358. https://doi.org/10.1161/CIRCINTERVENTIONS.109.873703.

(61) Jaschke, B.; Michaelis, C.; Milz, S.; Vogeser, M.; Mund, T.; Hengst, L.; Kastrati, A.; Schomig, A.; Wessely, R. Local Statin Therapy Differentially Interferes with Smooth Muscle and Endothelial Cell Proliferation and Reduces Neointima on a Drug-Eluting Stent Platform. *Cardiovasc. Res.* **2005**, *68* (3), 483–492. https://doi.org/10.1016/j.cardiores.2005.06.029.

(62) Zago, A. C.; Matte, B. S.; Reginato, L.; Iturry-Yamamoto, G.; Krepsky, A.; Bergoli, L. C. C.; Balvedi, J.; Raudales, J. C.; Saadi, E. K.; Zago, A. J. First-in-Man Study of Simvastatin-Eluting Stent in De Novo Coronary Lesions. *Circ. J.* **2012**, *76* (5), 1109–1114. https://doi.org/10.1253/circj.CJ-11-1125.

Supplementary data

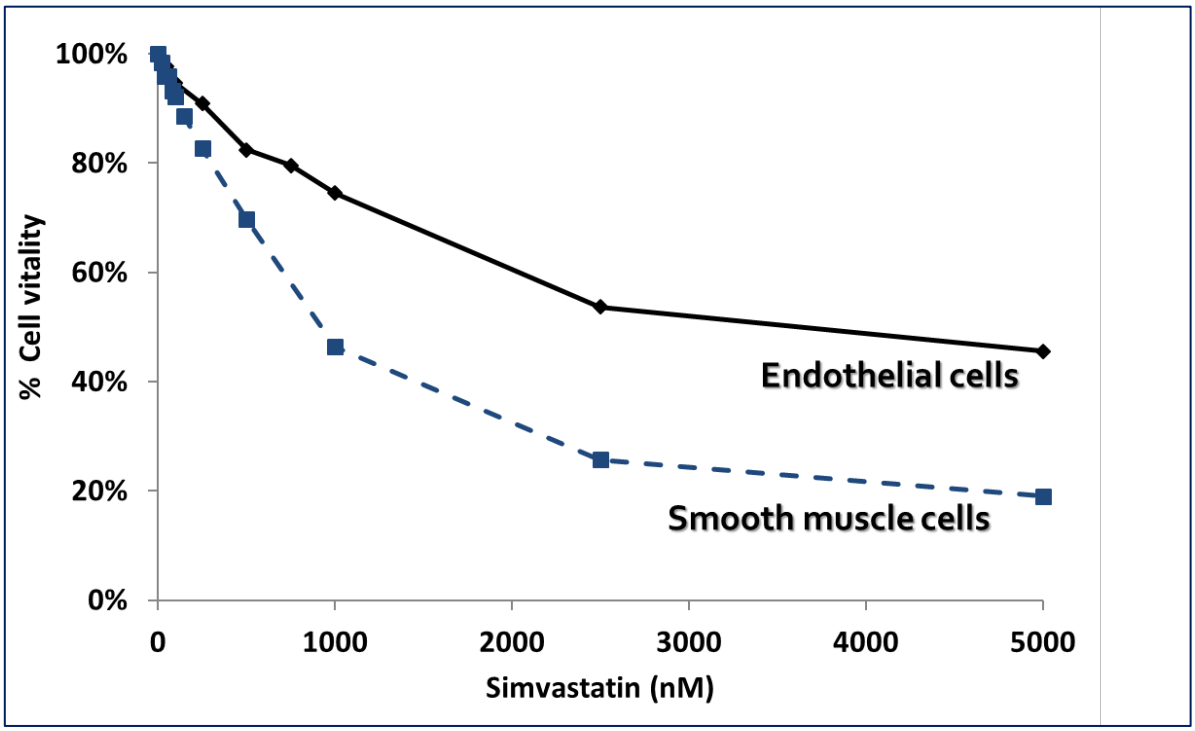

Figure S1: effect of SV concentration on Human Coronary Artery Endothelial Cells *(HCAEC) and* Human Coronary Artery Smooth Muscle *Cells (HCSMC) viability according to ISO/EN 10993-5 standard using the extraction method. Simvastatin shows a selectivity on both vascular cells lines in the range of 750 – 1500 nM*